



ELSEVIER

Journal of Molecular Liquids 111 (2004) 53–60

 journal of
**MOLECULAR
 LIQUIDS**
www.elsevier.com/locate/molliq

Temperature and pressure dependences of the structural dynamics: an interpretation of Vogel–Fulcher behavior in terms of the Adam–Gibbs model

 R. Casalini^{a,b,*}, M. Paluch^{a,c}, T. Psurek^c, C.M. Roland^a
^aNaval Research Laboratory, Chemistry Division, Code 6120, Washington DC 20375-5342, USA

^bGeorge Mason University, Chemistry Department, Fairfax, VA, USA

^cInstitute of Physics, Silesian University, Uniwersytecka 4, 40-007 Katowice, Poland

Received 25 February 2003; accepted 7 September 2003

Abstract

Dielectric measurements on 4,4'-methylenebis(*N,N*-diglycidylaniline) were carried out over a temperature range from 258 to 335 K, at hydrostatic pressures from ambient to 300 MPa. Both the shape of the α -relaxation function and the T_g -normalized temperature dependence of the relaxation times (fragility) were found to be independent of pressure, consistent with the established correlation between these two quantities. Interpretation of the data using an extension of the model of Adam and Gibbs yielded values for the configurational entropy and the excess heat capacity. The implication of this analysis is that these two quantities govern to a substantial extent both the temperature- and pressure-dependences of the structural relaxation times. We also show that all relaxation times can be rescaled onto a single master curve, whose abscissa is simply related to the ratio between the configurational entropy and the excess heat capacity.

© 2003 Elsevier B.V. All rights reserved.

Keywords: Glass transition; Dielectric relaxation; High pressure

1. Introduction

When cooled at a sufficiently high rate, most liquids retain their disordered structure while progressively transforming into a solid state, the glassy state. This ubiquitous and complex process has been studied for many decades, but nevertheless remains a topic of current scientific debate. By observing the molecular motions with a variety of experimental techniques, it has been observed that these became progressively slower, with characteristic times going from nanoseconds to times that exceed the normal duration of experiments, so that the system is actually in non-equilibrium.

Among the experimental techniques used to probe the dynamical properties of supercooled liquids, dielectric spectroscopy is an especially useful method, since the dynamics can be probed over a very broad frequency range [1,2]. Dielectric relaxation measurements can also

be carried out over wide ranges of temperature and pressure, providing stern tests of models of the glass transition [3–7].

Dielectric loss spectra are often analyzed as a superposition of Havriliak–Negami functions [8]

$$\begin{aligned}
 \varepsilon''(\omega) &= \frac{\Delta\varepsilon \sin(\beta_{\text{HN}}\psi)}{\left[1 + 2(\omega\tau_{\text{HN}})^{\alpha_{\text{HN}}}\cos(\pi\alpha_{\text{HN}}/2) + (\omega\tau_{\text{HN}})^{2\alpha_{\text{HN}}}\right]^{\beta_{\text{HN}}/2}} \psi \\
 &= \arctan \frac{(\omega\tau_{\text{HN}})^{\alpha_{\text{HN}}}\sin(\pi\alpha_{\text{HN}}/2)}{1 + (\omega\tau_{\text{HN}})^{\alpha_{\text{HN}}}\cos(\pi\alpha_{\text{HN}}/2)}
 \end{aligned}
 \tag{1}$$

where $\Delta\varepsilon$ is the dielectric strength, τ_{HN} the relaxation time, ω the angular frequency, and α_{HN} and β_{HN} are shape parameters. The latter yield the exponents, $\alpha_{\text{HN}} \times \beta_{\text{HN}}$ and α_{HN} , of the respective power laws describing the high and low frequency flanks of the

*Corresponding author.

 E-mail address: casalini@ccs.nrl.navy.mil (R. Casalini).

dielectric loss peak. In the analysis of the dynamics, it is common to utilize the model-independent relaxation time defined as the inverse of the angular frequency of the maximum in the dielectric loss, $\tau = 1/\omega_{\max}$. This can be obtained either directly from the spectra, or calculated from τ_{HN} [9]

$$\tau_{\text{HN}} = 2\pi \times \tau \left[\tan \left(\frac{\pi}{2(\beta_{\text{HN}} + 1)} \right) \right]^{1/\alpha_{\text{HN}}} \quad (2)$$

The latter is necessary if more than one relaxation (or DC conductivity) must be accounted for.

The temperature behavior of the relaxation time for many glass formers can be described by the Vogel–Fulcher (VF) [10,11] equation

$$\tau(T) = \tau_0 \exp \left(\frac{DT_0}{T - T_0} \right) \quad (3)$$

where T is the absolute temperature, T_0 the Vogel temperature and D the fragility parameter. Deviations from VF behavior are seen for small τ ($\tau \sim 10^{-6}$ s) [12].

A phenomenological extension of the VF equation has been found to describe the pressure-dependence of different glass-formers [13,14]

$$\tau(P) = \tau_P \exp \left(\frac{D_P P}{P_0 - P} \right) \quad (4)$$

where P is the pressure, τ_P can be obtained from isobaric data at atmospheric pressure,

P_0 denotes the pressure at which τ diverges and D_P can be referred to, for consistency, as the pressure fragility parameter [15].

Of the different theoretical models proposed for interpreting the slowing down of the dynamics upon approach of the glass transition, much effort has been directed to the model of Adam and Gibbs (AG) [16], which predicts

$$\tau = \tau_{\text{AG}} \exp \left(\frac{A}{TS_c} \right) \quad (5)$$

where S_c is the configurational entropy, A is a constant related to the intermolecular potential and τ_{AG} is the relaxation time in the limit of high temperatures. The important result of this model is establishing a link between the dynamics (τ) and thermodynamical quantities (S_c). It is noteworthy that Eq. (5) has been found to be valid for simulations [17,18], which arise from a different theoretical approach than used originally by AG. Also, variants have been proposed to the original model to establish links between Eq. (5) and the molecular dynamics [19].

The operative definition proposed by AG to determine S_c is to consider it equal to the excess entropy, S_{ex} , of the melt with respect to the crystal. As pointed out by Goldstein [20] very many years ago, however, this definition is problematic, because S_{ex} may include vibrational terms, with consequent overestimate of S_c . This point has recently been emphasized by Johari [21]. Nevertheless, tests of the AG using S_{ex} have been successful for temperatures not too far from T_g [22–25] presumably reflecting a proportionality between S_c and S_{ex} [26], as found by computer simulations [27,28]. In this approximation, it follows that

$$S_c(T, P) = \Delta S_{\text{fus}} + \int_{T_k}^T \frac{\Delta C_p(T')}{T'} dT' - \int_0^P \Delta \left(\frac{\partial V}{\partial T} \right)_{P'} dP' \quad (6)$$

where ΔS_{fus} is the entropy of fusion and T_k , the Kauzmann temperature, is the ideal temperature of vanishing S_c . In this work is assumed $T_k = T_0$ (the Vogel temperature). The first integral is related to the excess molar heat capacity, $\Delta C_p = C_p^{\text{melt}} - C_p^{\text{crystal}}$, of the melt relative to the crystal, and the second integral can be expressed in terms of the excess molar thermal expansion,

$\Delta \left(\frac{\partial V}{\partial T} \right)_{P'} = \left(\frac{\partial \Delta V}{\partial T} \right)_{P'} = \left(\frac{\partial (V^{\text{melt}} - V^{\text{crystal}})}{\partial T} \right)_{P'}$. At atmospheric pressure ($P \sim 0$), the second integral is zero, and since the temperature dependence of the excess heat capacity can be described over a limited range by $\Delta C_p(T) = k/T$, then $S_c(T) = S_\infty - k/T$, where k is a constant and S_∞ is the limit of S_c at very high temperatures [25]. By substituting this equation into Eq. (5), the VF expression (Eq. Eq. (3)) is obtained, where T_0 is the Vogel temperature ($T_0 = k/S_\infty$) and D ($D = C/k$) is the fragility parameter. At pressures above atmospheric, the second integral of Eq. (6), describing the isothermal reduction of S_c , is non-negligible. By substituting Eq. (6) in Eq. (5), a VF-like equation for $\tau(T, P)$ is again obtained, with the Vogel temperature now defined as [29]

$$T_0^*(T, P) = \frac{T_0}{1 - \frac{1}{S_\infty} \int_0^P \Delta \left(\frac{\partial V}{\partial T} \right)_{P'} dP'} \quad (7)$$

However, this result should be considered an approximation, relying on the assumption of proportionality between of S_c and S_{ex} , for both the isobaric and isothermal terms in Eq. (6). A more rigorous analysis would require data on the crystal properties, which are lacking. Further discussion of the proportionality between S_c and S_{ex} and a modified version of Eq. (7) can be found in a recent paper [30]. To arrive at a more

accessible form for T_0^* , the integral in Eq. (7) was calculated using the Tait equation [31–33] to describe the temperature and pressure dependence of the volume, $V(T,P) = V(T,0)[1 - C \ln(1 + P/B(T))]$, where C is a constant (average value $C = 8.92 \times 10^{-2}$) and $B(T)$ has the dimensions of pressure [33,34]. The temperature dependence of $B(T)$ is well described by $B(T) = b_1 \exp(-b_2 T)$, with typical values $b_1 = 900$ MPa and $b_2 = 4 \times 10^{-3} \text{ K}^{-1}$ [33,34]. Using this procedure the following expression for T_0^* was derived [5]

$$T_0^*(T,P) = \frac{T_0}{1 + \left(\frac{\delta}{S_\infty}\right)} \left\{ -(\beta + \gamma - 1)P + [(\gamma - 1)B(T) + \gamma P] \ln\left(1 + \frac{P}{B(T)}\right) \right\} \quad (8)$$

in which $\delta = CV^{\text{melt}}(T,0)b_2$, $\beta = \delta^{-1} \Delta(\partial V/\partial T)_{P=0}$ and $\gamma = \alpha/b_2$ with α being the thermal expansion coefficient of the melt. As pressure goes to zero, T_0^* becomes T_0 .

According to this approach, the fragility parameter D is independent of pressure (assuming the free energy barrier to rearrangements remains constant). As a consequence, if the temperature dependence of the excess expansivity integral is negligible, T_0^* depends only on pressure, and $\tau(T,P)$ data at a fixed pressure should be described by a VF equation having the same fragility parameter D . Moreover, it follows in turn that if T_g/T_0^* and D are both independent of pressure, then the fragility (e.g. steepness index, $m_T = d \log(\tau)/d(T/T_g)|_{T=T_g}$ [35]) is independent of pressure [36]. It has been shown that T_0^* is sensibly independent of pressure when the investigated temperature range is less than $1/b_2$ and that $P < B(T)$ [35].

In comparing the phenomenological Eq. (4) and the extended AG model, it is evident that the former has a higher number of free parameters (four vs. two) in order to include a description of the pressure dependence of the relaxation times. Moreover, the AG approach is not phenomenological, and these parameters can be all related to physical properties of the material. In fact, all these parameters can be determined a priori from the properties of melt and crystal, although in practice the available properties for the melt reduces the adjustable parameters to just one [37].

In this paper, we present dielectric results, obtained as a function of both temperature and pressure, for 4,4'-methylene-bis(*N,N*-diglycidylaniline). Our purpose is to study the structural relaxation properties, and in particular compare the results obtained from the extended AG model with those obtained using the more phenomenological approach. This epoxy is particularly well-suited for such an investigation, since its structural relaxation

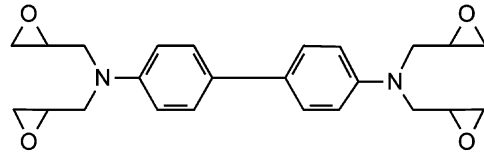


Fig. 1. Molecular structure of 4,4'-methylenebis(*N,N*-diglycidylaniline), referred to herein as MBDA.

is very sensitive to both pressure and temperature ($m_T > 100$), and crystallization is not a complicating factor.

2. Experimental

The molecular structure of 4,4'-methylene-bis(*N,N*-diglycidylaniline) (Aldrich Chemical), referred to herein as MBDA, is displayed in Fig. 1. The material was used as received. Dielectric measurements were carried out using a Novocontrol GmbH Alpha dielectric spectrometer. For ambient pressure measurements, the sample was contained in a parallel plate cell (diameter 10-mm, gap 0.1 mm). Temperature was controlled using a nitrogen-gas cryostat, with temperature stability better than 0.1 K. High pressure measurements employed equipment described in detail elsewhere [38]. The sample was contained between two plates, with pressure exerted via silicone fluid, using a piston in contact with a hydraulic press. The pressure was measured by a Nova Swiss tensometric pressure meter (resolution = 0.1 MPa). The temperature was controlled by a thermostatic bath to within 0.1 K.

3. Results and discussion

Observed at lower frequencies in the dielectric loss spectra of MBDA (Fig. 2) is the DC conductivity, σ_{DC} , which decreases rapidly with decreasing temperature and increasing pressure. This conductivity can be accounted for by an additional term in Eq. (1), $\varepsilon'' = \sigma_{DC}(\omega \varepsilon_0)^{-1}$, where ε_0 is the vacuum permittivity. At higher frequency, the structural (or α -) relaxation peak is evident. At still higher frequency, another contribution arises, a secondary relaxation seen in other epoxy systems [39–41]. This secondary process, which is visible only in the lower temperature spectra in Fig. 2, is believed to be due to non-cooperative reorientation of the terminal epoxy groups. Note that below T_g , there occurs another process, at frequencies intermediate between the structural and the secondary relaxation. Its amplitude is about two orders of magnitude smaller than that of the α -process. This sub- T_g process, which has the characteristics of a Johari–Goldstein relaxation [42], is not seen in Fig. 2, which includes only measurements above T_g . In this paper, we restrict our attention to the dynamics of the α -relaxation.

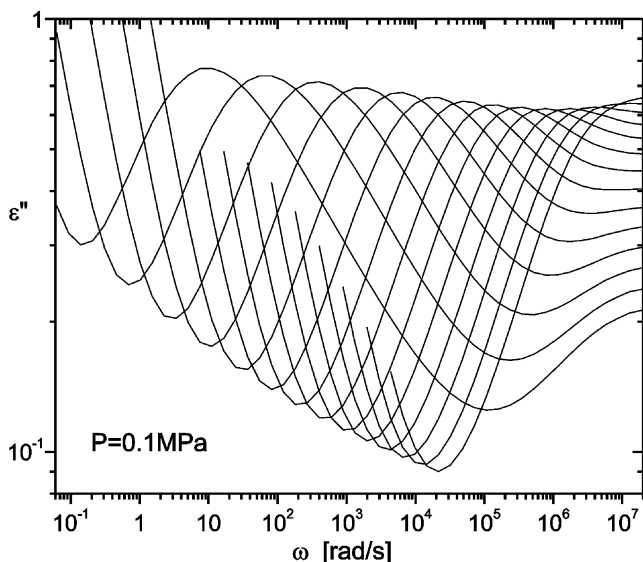


Fig. 2. Dielectric loss spectra of MBDA at ambient pressure and (from left to right) $T=264, 267, 270, 273, 276, 279, 282, 285, 288, 291, 294, 297, 300$ and 303 K.

Fig. 3 shows a master plot of $\varepsilon''(\omega)/\varepsilon''_{\max}$ vs. $\log(\omega/\omega_{\max})$ for spectra measured at $T=287.6$ K and various pressures. The shape of the α peak is essentially independent of pressure. Analogous results are obtained by varying the temperature at fixed pressure. In the inset to Fig. 3 are shown the power law exponents, obtained from fitting the spectra to Eq. (1). It is worth noting that this spectral invariance to both temperature and

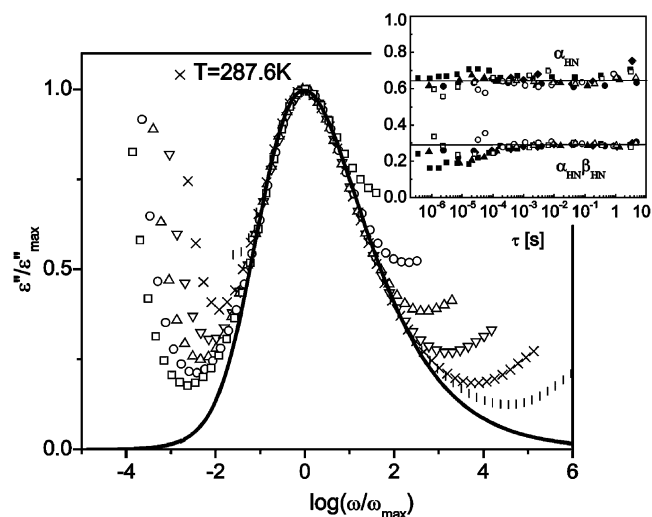


Fig. 3. Master plot of data measured at $T=287.6$ K and $P=12.5$ (\square), 38.7 (\circ), 66.3 (\triangle), 94.4 (∇), 120.5 (\times) and 145.2 MPa (\diamond). The inset shows the shape parameters as a function of the relaxation time, obtained from fits of the spectra to Eq. (1), with the inclusion of a σ_{DC} term and a fractional power law contribution at high frequency (to account for the secondary relaxation). These data are the four isobars at $P=0.1$ (\blacksquare), 100 (\bullet), 200 (\blacktriangle) and 300 MPa (\blacklozenge), and the three isotherms at $T=277.3$ (\triangle), 287.1 (\circ) and 298.1 K (\square). The solid line is the Fourier transform of $\Phi(t)$ with $\beta_{KWW}=0.37$.

pressure has been found for the α -relaxation in other epoxies near their glass transition [43–45].

From the dielectric spectra, measured over 80° and a 240 MPa range of pressures, we obtain the relaxation

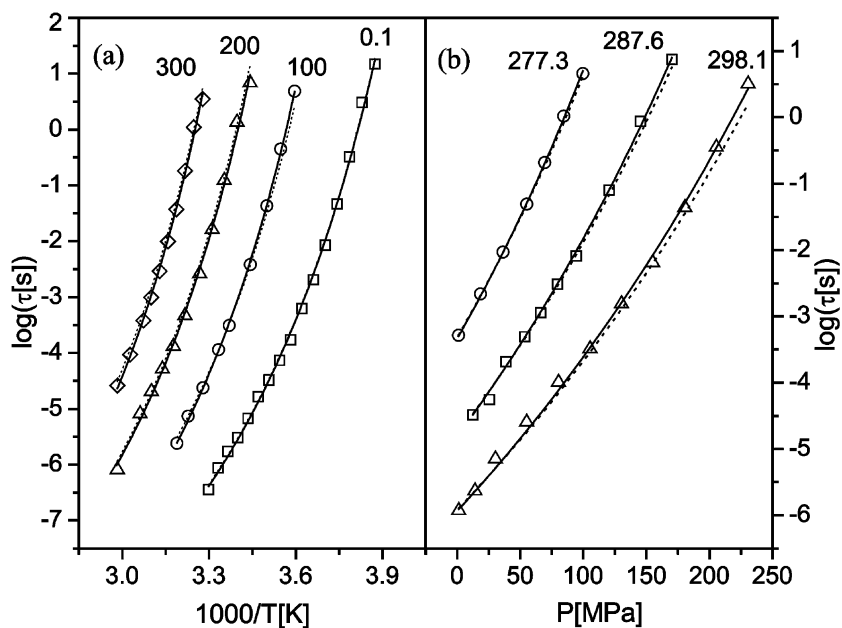


Fig. 4. α -relaxation times (a) measured at four pressures (as indicated in the figure in MPa) as a function of reciprocal temperature and (b) measured at three temperatures (as indicated in Kelvin) as a function of the pressure. The solid lines are the fit using Eq. (3) in (a) and Eq. (4) in (b) and the dotted lines the fit to the AG model (Eq. (3) with T_0 substituted by T_0^* like in Eq. (8)).

Table 1
Results of fitting the relaxation times in Fig. 4a to Eq. (3)

P (MPa)	D	T_0 (K)	$\log(\tau_0(\text{s}))$
1	7.1 ± 0.8	214.3 ± 2.9	-13.8 ± 0.5
100	7.2 ± 1.6	229.6 ± 5.8	-14.2 ± 1.1
200	7.4 ± 1.2	239.3 ± 4.8	-14.0 ± 0.8
300	7.3 ± 2.2	251.1 ± 8.5	-14.1 ± 1.6

time over more than 7 decades. In Fig. 4a, these are shown as a function of inverse temperature, for representative pressures (0.1, 100, 200 and 300 MPa). Curves calculated using Eq. (3) are shown as solid lines, with the fitting parameters listed in Table 1. To quantify the rapidity of the variation of τ with temperature, we calculate the steepness index (for $\tau(T_g)=100$ s),

$$m_T = \frac{DT_0}{T_g \ln(10)} \left(1 - \frac{T_0}{T_g}\right)^{-2} \quad (9)$$

These results, shown in Fig. 5 (solid symbols), make evident the constancy of the fragility with respect to pressure, at least over the investigated range. The value of m_T for MBDA is comparable to that of other epoxy compounds: poly[phenyl glycidyl ether-*co*-formaldehyde] (PPGE) $m_T=95$ [42], diglycidyl ether of bisphenol-A (DGEBA) $m_T=105$ [42] and triphenylmethane triglycidyl ether (TPTE) [40] $m_T=106$. Also close to that of other well known glass formers ortho-terphenyl $m_T=81$ [35] propylene carbonate $m_T=104$ [35], triphenyl-phosphite $m_T=115$ [46] and toluene $m_T=122$ [47].

Fragility for many glass formers has been found to correlate with the breadth of the structural relaxation [35]. For example, by fitting the α peak to the one-sided Fourier transform of the Kohlraush–Williams–Watts (KWW) [48,49] stretched exponential function

$$\Phi(t) = \exp\left[-(t/\tau_{\text{KWW}})^{\beta_{\text{KWW}}}\right] \quad (10)$$

where the fractional exponent $0 < \beta_{\text{KWW}} \leq 1$, the following relation is found [35]

$$m_T = 250 \pm 30 - 320\beta_{\text{KWW}} \quad (11)$$

Fig. 3 shows the transform of $\Phi(t)$ with $\beta_{\text{KWW}}=0.37$ (solid line), which gives a quite good description of the α relaxation. Eq. (11) then yields $m_T=130 \pm 30$, which agrees, in the limit of the experimental error, with the value of m_T determined in Fig. 5.

In Fig. 4b, we show τ as a function of pressure for three temperatures (278.1, 387.1 and 397.1 K), along with the fit to Eq. (4) (solid lines), with D , T_0 and τ_0 determined from the data for $P=0.1$ MPa. The parameter D_p is assumed to be independent of temperature. The results are listed in Table 2.

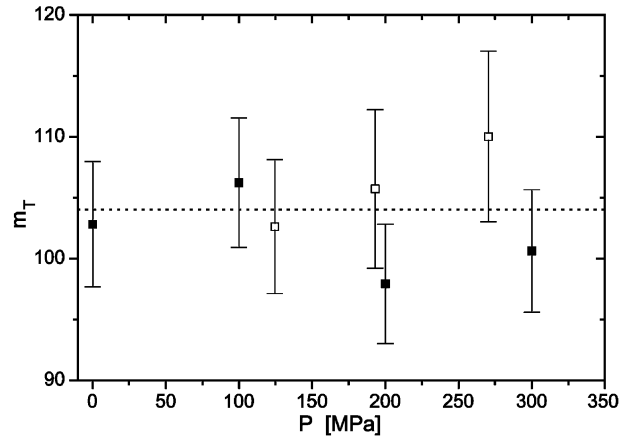


Fig. 5. Steepness index deduced from measurements at constant pressure using Eq. (9) (solid symbols) and from measurements at constant temperature using Eq. (12) (open symbols). The dotted line represents the mean value, $m_T=104 \pm 4$.

From the isothermal measurements, the steepness index can be calculated from the relationship [14]

$$m_T = T \left(\frac{\partial \log(\tau)}{\partial P} \right) \left(\frac{\partial T_g}{\partial P} \right)^{-1} \quad (12)$$

The pressure dependence of the glass temperature determined from the measurements at both constant pressure and constant temperature is displayed in Fig. 6. The solid line represents the fit of a second-order polynomial, yielding 256.7 ± 0.7 K, $(1.8 \pm 0.1) \times 10^{-1}$ K/MPa and $(-1.3 \pm 0.3) \times 10^{-4}$ K/MPa² for the respective coefficients. The value of $dT_g/dP=180$ K/GPa at ambient pressure is higher than the values determined for other epoxies compounds: PPGE $dT_g/dP=154$ K/GPa [44] TPTE $dT_g/dP=167$ K/GPa [7] and poly[bisphenol A-*co*-epichlorohydrin], glycidyl end-capped $dT_g/dP=156$ K/GPa [50].

The parameters for the pressure dependence of T_g were used in Eq. (12) to calculate the pressure derivative of T_g . The obtained m_T are shown as the open symbols in Fig. 5, where their consistency with the m_T , as deduced from measurements at constant pressure, can be observed. Fig. 5 shows that, within the limit of the experimental error, the fragility is independent of pressure.

Table 2
Fitting parameters (Eq. (4)) for the relaxation times in Fig. 4b

T (K)	D_p	P_0 (MPa)
298.1	44 ± 3	922 ± 57
287.6	44 ± 3	740 ± 47
277.3	44 ± 3	571 ± 38

D , T_0 and τ_0 were fixed at the values determined for $P=0.1$ MPa. The parameter D_p was shared between the three data sets.

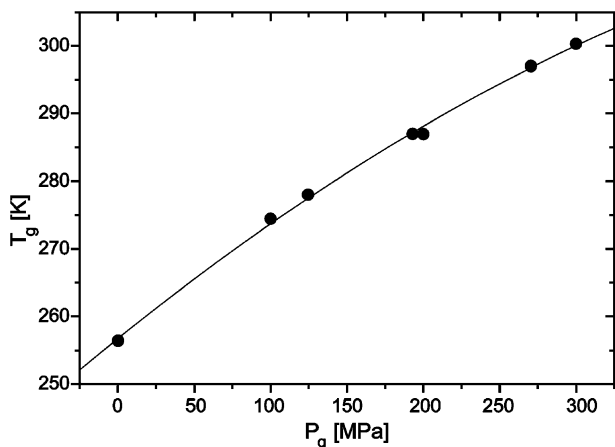


Fig. 6. Glass temperatures determined from measurements at constant temperature (Fig. 4b) and at constant pressure (Fig. 4a). The solid line represents a second order polynomial.

Since fragility is expected to be correlated with the breadth of the α -relaxation function [35,51], the observed independence of m_T to pressure is consistent with the invariance of the shape of the α -relaxation to pressure (Fig. 3). That is, for MBDA the correlation expressed by Eq. (11) is maintained at elevated pressure, as found previously for other glass-formers [36,52]. This suggests that the influence of temperature and pressure on the intermolecular cooperativity governing the local dynamics is qualitatively the same.

To the extent this fragility and the related non-exponentiality of the relaxation function reflect chemical structure (e.g. through steric and other intermolecular interactions [53]), our results indicate that over the present range of pressures, there is no alteration of the intermolecular potential. Such behavior conforms to the idea underlying the AG model, that the slowing down of molecular motion is dominated by a decrease of the number of configuration available to the system, without change of the intermolecular interactions per se.

Fig. 7 demonstrates the congruent behavior of the two Vogel parameters, $T_0(P)$ and $P_0(T)$. This result may be surprising, since Eq. (4) derives from Eq. (3) only by the ad hoc replacement of T with the reciprocal of P . However, the consistency reflects the fact that in both cases, these represent the conditions under which the relaxation time diverges.

The phenomenological analysis presented above brings out the main characteristics of structural relaxation in MBDA. We have noted that the independence of the shape parameter and fragility to pressure is consistent with the AG model. Thus, it is of interest to examine the $\tau(T, P)$ using Eq. (8) (in combination with the VF equation), and assess whether the obtained parameters are consistent with the known physical properties of MBDA and other epoxy systems. As already discussed,

the function T_0^* is determined from the integral of the molar excess thermal expansivity of the melt with respect to the crystal [5]. The temperature dependence of this integral is very weak, and in particular at low pressures ($P < 0.2$ MPa) deviations smaller than 0.3% are expected [29]. Accordingly, we assume T_0^* depends only on pressure.

The analysis of $\tau(T, P)$ in terms of the AG model was thus carried out using Eq. (3), with T_0 replaced by T_0^* (Eq. (8)). As shown elsewhere [37,54], the parameters in Eq. (5) can be independently determined from PVT data. In the present case, we use results for TPTE (having very similar values of dT_g/dP and m_T) [7], $B = 1170$ MPa, $\gamma = 0.12$ and $\delta = 1.3 \times 10^{-7} \text{ m}^3 \text{ mol}^{-1} \text{ K}^{-1}$ (the latter calculated from the density $= 1.15 \text{ gmol}^{-1}$ and molecular weight $= 422.53 \text{ gmol}^{-1}$ of MBDA), together with the parameters deduced from the VF fit to the atmospheric pressure measurements (Table 1). The simultaneous fits of the seven sets of $\tau(T, P)$ data are shown in Fig. 4 (dotted lines), yielding for the two adjustable parameters $\beta = 1.01 \pm 0.07$ and $S_\infty = 184 \pm 18 \text{ Jmol}^{-1} \text{ K}^{-1}$. An independent assessment of these parameters from other measurements is not currently possible for MBDA. However, this S_∞ is close to values obtained using calorimetry and dielectric data for PPGE $S_\infty = 229 \pm 2 \text{ Jmol}^{-1} \text{ K}^{-1}$ and DGEBA $S_\infty = 233 \pm 1 \text{ Jmol}^{-1} \text{ K}^{-1}$ [37].

The respective fits using the extended AG and the VF models (Fig. 4) are quite close, although the former was more constrained due to the simultaneous fitting of all the seven data sets with a unique set of parameters. Both models predict a temperature (T_0) or pressure (P_0) at which τ diverges. In Fig. 7, the values of T_0 and P_0

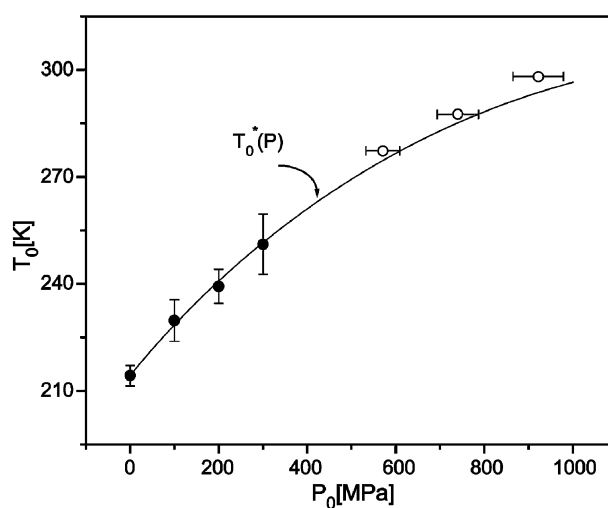


Fig. 7. Vogel temperature from measurements at constant pressure (open symbols) and at constant temperature (solid symbols), using the phenomenological VF equation (Eq. (3)). The solid line is the function $T_0^*(P)$ calculated from Eq. (5), using the parameters obtained from the fit of the $\tau(T, P)$ data to the AG model.

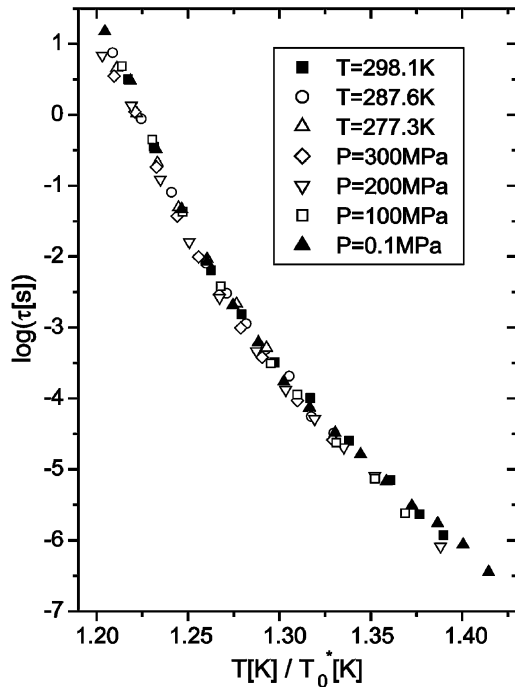


Fig. 8. Master curve of the α -relaxation times vs. T/T_0^* , where T_0^* is calculated from Eq. (5) using the fit parameters from the AG model.

deduced from the VF equation are compared to the results from the AG model; there is no significant difference. These results indicate that the phenomenological VF approach (Eqs. (3) and (4)) can be reproduced and interpreted in the framework of the AG model.

Using the result of the extended AG model it is possible to plot the relaxation times vs. the quantity T/T_0^* , which enables rescaling of all the isothermal and isobaric data onto a single master plot (Fig. 8). Note that this ratio can be expressed as

$$\frac{T}{T_0^*(T,P)} = \frac{S_c(T,P)}{\Delta C_p(T,P=0)} - 1 \quad (13)$$

where S_c is the configurational entropy and ΔC_p the excess heat capacity ($P=0$ indicates ambient pressure). Thus, the function T/T_0^* is a well-defined thermodynamic quantity (within the limits of the definition of S_c), playing a central role in the description of the temperature and pressure dependence of the structural dynamics. We also point out that the fragility can be related to the ratio $S_c/\Delta C_p$. By defining $m_{T_{\min}} = \log(\tau(T_g)/\tau_0)$ from Eq. (12), it follows that

$$\frac{m_T}{m_{T_{\min}}} = 1 + \left. \frac{\Delta C_p(T,P=0)}{S_c(T,P)} \right|_{T_g} \quad (14)$$

The correlation implied by this expression has recently

been verified, at least at ambient pressure, for several glass formers [55].

4. Conclusions

Dielectric measurements on 4,4'-methylenebis(*N,N*-diglycidylaniline), a high functionality epoxy, were carried out over a wide range of temperature and pressure. The behavior of the structural relaxation was analyzed using a phenomenological approach. The shape of the α -relaxation was found to be independent of both temperature and pressure (Fig. 3). Moreover, from fitting the $\tau(T,P)$ data to the extended VF equation (Eq. (4)), the fragility was shown to be independent of pressure. This behavior is consistent with the known correlation between these properties, and suggests that the increased intermolecular cooperativity, responsible for the slowing down of the molecular motions, has the same origin, whether brought about by decreasing temperature or increasing pressure.

The data were also analyzed using the AG model, relating the dynamics to the magnitude of the configurational entropy and the excess heat capacity. The implication is that the ratio of these two quantities governs the fragility, as well as both the temperature- and pressure-dependences of τ . Moreover, the results of the AG analysis are consistent with the phenomenological VF function (i.e. T_0 vs. P_0 curve, and independence of the α -relaxation shape and its fragility from pressure,) allowing an interpretation of the results obtained with such approach. In fact, the more stringent AG analysis, using Eq. (5) (in combination with the VF equation), describes the relaxation times equally well. Finally, we show that the AG model can be the basis for a rescaling of the relaxation times onto a single master curve, in which the abscissa is expressed in terms of the configurational entropy and the excess heat capacity.

Acknowledgments

The work at NRL was supported by the Office of Naval Research. M. Paluch acknowledges financial support from the State Committee for Scientific Research (KBN; Poland) under Project No. 5PO3B 022 20.

References

- [1] P. Lunkenheimer, Dielectric Spectroscopy of Glassy Dynamics, Shaker, Aachen, 1999.
- [2] P. Lunkenheimer, U. Schneider, R. Brand, A. Loidl, *Contemp. Phys.* 41 (2000) 15.
- [3] (a) G. Williams, *Trans. Faraday Soc.* 60 (1964) 1556
(b) G. Williams, *ibid* 60 (1964) 1548
(c) G. Williams, *ibid* 61 (1965) 1564
(d) G. Williams, *ibid* 62 (1966) 2091.
- [4] S. Corezzi, S. Capaccioli, R. Casalini, D. Fioretto, M. Paluch, P.A. Rolla, *Chem. Phys. Lett.* 320 (2000) 113.

- [5] R. Casalini, S. Capaccioli, M. Lucchesi, P.A. Rolla, S. Corezzi, *Phys. Rev. E* 63 (2001) 031207.
- [6] M. Paluch, S. Hensel-Bielowka, T. Psurek, *J. Chem. Phys.* 113 (2000) 4374.
- [7] M. Paluch, *J. Chem. Phys.* 115 (2001) 10 029.
- [8] S. Havriliak, S.J. Negami, *Polym. Sci. Polym. Symp.* 14 (1966) 89.
- [9] F. Alvarez, A. Alegria, J. Colmenero, *Phys. Rev. B* 44 (1991) 7306.
- [10] H. Vogel, *Phys. Z* 22 (1921) 645.
- [11] G.S. Fulcher, *J. Am. Ceram. Soc.* 8 (1923) 339.
- [12] F. Stickel, Thesis, Johannes Gutenberg-Universität Mainz, 1995.
- [13] M. Paluch, A. Patkowski, E.W. Fischer, *Phys. Rev. Lett.* 85 (2000) 2140.
- [14] M. Paluch, J. Gapinski, A. Patkowski, E.W. Fischer, *J. Chem. Phys.* 114 (2001) 8048.
- [15] I.M. Hodge, *J. Non-Cryst. Solids* 202 (1996) 164.
- [16] G. Adam, J.H. Gibbs, *J. Chem. Phys.* 43 (1965) 139.
- [17] S. Sastry, *Nature* 409 (2001) 164.
- [18] F. Sciortino, W. Kob, P. Tartaglia, *Phys. Rev. Lett.* 83 (1999) 3214.
- [19] H. Huth, M. Beiner, E. Donth, *Phys. Rev. B* 61 (2000) 15 092.
- [20] M. Goldstein, *J. Chem. Phys.* 64 (1975) 4767.
- [21] G.P. Johari, *J. Chem. Phys.* 112 (2000) 8958.
- [22] J.H. Magill, *J. Chem. Phys.* 47 (1967) 4802.
- [23] S. Takahara, O. Yamamuro, H. Suga, *J. Non-Cryst. Solids* 171 (1994) 259.
- [24] S. Takahara, O. Yamamuro, T. Matsuo, *J. Phys. Chem.* 99 (1995) 9580.
- [25] R. Richert, C.A. Angell, *J. Chem. Phys.* 108 (1998) 9016.
- [26] L.M. Martinez, C.A. Angell, *Nature* 410 (2000) 663.
- [27] F.W. Starr, S. Sastry, E. LaNave, A. Scala, H.E. Stanley, F. Sciortino, *Phys. Rev. E* 63 (2001) 041201.
- [28] S. Kamath, R.H. Colby, S.K. Kumar, J. Bashnagel, *J. Chem. Phys.* 116 (2002) 865.
- [29] S. Capaccioli, M. Lucchesi, R. Casalini, S. Presto, P.A. Rolla, M.T. Viciosa, S. Corezzi, D. Fioretto, *Philos. Mag. B* 82 (2002) 652.
- [30] D. Prevosto, M. Lucchesi, S. Capaccioli, R. Casalini, P.A. Rolla, *Phys. Rev. B* 67 (2003) 174202.
- [31] P.G. Tait, *Phys. Chem.* 2 (1888) 1.
- [32] H. Schlosser, J. Ferrante, *J. Phys.: Condens. Matter.* 1 (1989) 2727.
- [33] D.W. VanKrevelen, *Properties of Polymers*, Elsevier, Amsterdam, 1997.
- [34] R. Simha, P.S. Wilson, O. Olabisi, *Kolloid-Z* 251 (1973) 402.
- [35] R. Böhmer, K.L. Ngai, C.A. Angell, D.J. Plazek, *J. Chem. Phys.* 99 (1993) 4201.
- [36] R. Casalini, M. Paluch, J.J. Fontanella, C.M. Roland, *J. Chem. Phys.* 117 (2002) 4091.
- [37] R. Casalini, S. Capaccioli, M. Lucchesi, M. Paluch, S. Corezzi, P.A. Rolla, *J. Non-Cryst. Solids* 307–310 (2002) 264.
- [38] P. Urbanowicz, S.J. Rzoska, M. Paluch, B. Sawicki, A. Szulc, J. Ziolo, *J. Chem. Phys.* 201 (1995) 575.
- [39] R. Casalini, D. Fioretto, A. Livi, M. Lucchesi, P.A. Rolla, *Phys. Rev. B* 56 (1997) 3016.
- [40] D. Pisignano, S. Capaccioli, R. Casalini, M. Lucchesi, P.A. Rolla, A. Justl, E. Rössler, *J. Phys.: Condens. Matter.* 13 (2001) 4405.
- [41] S. Capaccioli, R. Casalini, M. Lucchesi, G. Lovicu, D. Prevosto, D. Pisignano, G. Romano, P.A. Rolla, *J. Non-Cryst. Solids* 307–310 (2002) 238.
- [42] S. Corezzi, M. Beiner, H. Huth, K. Schröter, S. Capaccioli, R. Casalini, D. Fioretto, E. Donth, *J. Chem. Phys.* 117 (2002) 2435.
- [43] S. Corezzi, P.A. Rolla, M. Paluch, J. Ziolo, D. Fioretto, *Phys. Rev. E* 60 (1999) 4444.
- [44] M. Paluch, S. Hensel-Bielowka, J. Ziolo, *Phys. Rev. E* 61 (2000) 526.
- [45] T. Psurek, S. Hensel-Bielowka, J. Ziolo, M. Paluch, *J. Chem. Phys.* 116 (2002) 9882.
- [46] S. Dvinskikh, G. Benini, J. Senker, M. Vogel, J. Wiedersich, A. Kudlik, E. Rössler, *J. Phys. Chem. B* 103 (1999) 1727.
- [47] A. Kudlik, C. Tschirwitz, S. Benkhof, T. Blochowicz, E. Rössler, *Europhys. Lett.* 40 (1997) 649.
- [48] R. Kohlrausch, *Pogg. Ann. Phys. (III)* 12 (1847) 393.
- [49] G. Williams, D.C. Watts, *Trans. Faraday Soc.* 66 (1970) 80.
- [50] M. Paluch, S. Hensel-Bielowka, J. Ziolo, *J. Chem. Phys.* 110 (1999) 10 978.
- [51] D.J. Plazek, K.L. Ngai, *Macromolecules* 24 (1991) 1222.
- [52] M. Paluch, K.L. Ngai, S. Hensel-Bielowka, *J. Chem. Phys.* 114 (2001) 10 872.
- [53] K.L. Ngai, C.M. Roland, *Macromolecules* 26 (1993) 6824.
- [54] R. Casalini, S. Capaccioli, M. Lucchesi, P.A. Rolla, M. Paluch, S. Corezzi, D. Fioretto, *Phys. Rev. E* 64 (2001) 041504.
- [55] U. Mohanty, N. Craig, J. Fourkas, *J. Chem. Phys.* 114 (2001) 10 577.